



# Optics Letters

## Reconstruction of structured laser beams through a multimode fiber based on digital optical phase conjugation

CHAOJIE MA,<sup>1</sup>  JIANGLEI DI,<sup>1</sup>  YI ZHANG,<sup>1</sup> PENG LI,<sup>1</sup> FAJUN XIAO,<sup>1</sup>  KAIHUI LIU,<sup>2,4</sup>  
XUEDONG BAI,<sup>3</sup> AND JIANLIN ZHAO<sup>1,\*</sup>

<sup>1</sup>MOE Key Laboratory of Material Physics and Chemistry under Extraordinary Conditions, and Shaanxi Key Laboratory of Optical Information Technology, School of Science, Northwestern Polytechnical University, Xi'an 710072, China

<sup>2</sup>State Key Laboratory for Mesoscopic Physics, School of Physics, Peking University, Beijing 100871, China

<sup>3</sup>Institute of Physics, Chinese Academy of Sciences, Beijing 100080, China

<sup>4</sup>e-mail: khliu@pku.edu.cn

\*Corresponding author: jlzhao@nwpu.edu.cn

Received 27 May 2018; revised 15 June 2018; accepted 16 June 2018; posted 18 June 2018 (Doc. ID 332498); published 10 July 2018

The digital optical phase conjugation (DOPC) technique is being actively developed for optical focusing and imaging through or inside complex media. Due to its time-reversal nature, DOPC has been exploited to regenerate different intensity targets. However, whether the targets with three-dimensional information through complex media could be recovered has not been experimentally demonstrated, to the best of our knowledge. Here, we present a method to regenerate structured laser beams based on DOPC. Although only the phase of the original scattered wave is time reversed, the reconstruction of a quasi-Bessel beam and vortex beams through a multimode fiber (MMF) is demonstrated. The regenerated quasi-Bessel beam shows the features of sub-diffraction focusing and a longer depth of field with respect to a Gaussian beam. Moreover, the reconstruction of vortex beams shows the fidelity of DOPC both in amplitude and phase, which is demonstrated for the first time, to the best of our knowledge. We also prove that the reconstruction results of DOPC through the MMF are indeed phase conjugate to the original targets. We expect that these results could be useful in super-resolution imaging and optical micromanipulation through complex media, and further pave the way for achieving three-dimensional imaging based on DOPC. © 2018 Optical Society of America

**OCIS codes:** (290.4210) Multiple scattering; (070.5040) Phase conjugation; (090.1995) Digital holography; (070.6120) Spatial light modulators; (050.4865) Optical vortices.

<https://doi.org/10.1364/OL.43.003333>

When light propagates through complex media, such as biological tissues and white paint, the refractive index inhomogeneity causes multiple scattering events [1,2]. These events are usually seen as obstacles for optical focusing and imaging.

To overcome such obstacles, several wavefront shaping techniques have been proposed, including iterative wavefront shaping, optical phase conjugation (OPC), and transmission matrix measurement [3–10]. Among them, OPC with its time-reversal nature could acquire the optimum wavefront with a single-shot measurement instead of multiple measurements. There are two types of OPC: analog OPC and digital OPC (DOPC). Different from analog-OPC-based nonlinear crystals, DOPC is achieved by using a digital image sensor and spatial light modulator (SLM) [7]. Here, the sensor is used to acquire the scattered wave by using digital holography, and the SLM serves to generate the phase-conjugate wavefront. Compared with analog OPC, DOPC has several intrinsic advantages, including the higher phase conjugation reflectivity and flexibly adjustable phase conjugation wavefront.

The first implementation of DOPC for refocusing light through a turbid medium was reported by Cui and Yang [7]. Subsequently, this technique was applied to other static and even dynamic complex media, including biomedical tissues and multimode fibers (MMFs), for light refocusing, as well as imaging [8–18]. At present, the related theory of DOPC has been well described by a scattering transmission matrix and could be found in Refs. [7,15]. Despite the case of partial phase conjugation, DOPC has been demonstrated for recovering different intensity targets, for example, a two-dimensional image or Gaussian focused spot [7–18]. However, the reconstruction of three-dimensional targets or structured laser beams through complex media has not been demonstrated based on DOPC. Structured laser beams, such as non-diffracting beams and singular beams, exhibit novel properties and have enabled important applications in super-resolution imaging, optical micromanipulation, microfabrication, and so on [19–22]. Recently, the generation of a quasi-Bessel beam, one class of non-diffracting beams, through a scattering system was demonstrated based on iterative wavefront optimization [23]. The generated quasi-Bessel beam shows a smaller full

width at half-maximum (FWHM) and a longer depth of field with respect to a Gaussian beam. But it was not shown that other structured laser beams could be reconstructed. Based on the complete knowledge of transmission matrix, including amplitude, phase, and polarization information, a quasi-Bessel beam, vortex beams, and other structured laser beams were generated through a MMF. But the generation of structured laser beams is established on the cylindrical symmetry waveguide feature of the MMF, which is unsuitable for other types of complex media [24]. Impressively, a quasi-Bessel beam and other structured laser beams through a strongly scattering medium were generated by digital filtering in the Fourier domain of the measured transmission matrix [25]. In principle, arbitrary structured laser beams through multiply scattering media could be generated based on a vector transmission matrix, which might open new opportunities in some fields, such as super-resolution imaging and optical micromanipulation [24–26]. However, due to the need of multiple measurements, this method might not be feasible for generating structured laser beams through dynamic scattering media [15,16].

In this Letter, we exploit the time-reversal principle of DOPC, for the first time to the best of our knowledge, to regenerate structured laser beams through a MMF. When a quasi-Bessel beam is coupled into the MMF, we demonstrate that the phase-conjugate focus shows the features of sub-diffraction focusing and propagation invariant over a limited distance, characterized by quasi-Bessel beams. In addition, although only the phase of the original scattered wave is time reversed, we also demonstrate the reconstruction of vortex beams with topological charges (TCs) of 1 and 2 that are measured by using the astigmatic transformation method. These results could show the fidelity of DOPC both in amplitude and phase, as well as the potential of DOPC for achieving three-dimensional imaging through complex media. Moreover, by measuring astigmatic transformation patterns of the corresponding input vortex beams, we could also prove that the reconstruction results of DOPC through complex media are indeed phase conjugate to the input targets.

Figure 1 depicts the schematic of the DOPC system for regenerating structured laser beams. The laser beam from a diode-pumped solid-state laser with a wavelength of 532 nm is expanded and collimated via a microscope objective  $MO_1$  (Newport, M-20X), pinhole, and Lens  $L_1$ . The collimated beam passes through a half-wave plate and then is split into a probe beam and a reference beam by a polarizing beam

splitter. The probe beam travels through a module, consisting of a mask and Lenses  $L_4$  and  $L_5$ , which is highlighted with a red dashed rectangle, to produce structured laser beams. In this module, the mask located in the back focal plane of  $L_4$  is used to modulate the probe beam. The modulated beam is imaged on the back focal plane of the microscope objective  $MO_2$  (Newport, M-20X) via the  $4f$  system composed of Lenses  $L_4$  and  $L_5$  and then coupled into a step index MMF (105  $\mu\text{m}$  core diameter,  $NA = 0.22 \pm 0.02$ ). Due to modal scrambling, the speckle field generated at the output facet of the fiber is collected and imaged on the complementary metal oxide semiconductor (CMOS) (MotionBLITZ EoSens Cube7) target through a microscope objective  $MO_3$  (Newport, M-40 $\times$ ) and Lens  $L_6$ . The reference beam is incident on a reflective phase-only SLM (Pluto-Vis, Holoeye) to achieve phase-only modulation. The SLM plane is directly imaged on the CMOS target via a  $4f$  system composed of Lenses  $L_2$  and  $L_3$ , which could address the precise alignments between the SLM and CMOS [14,27]. The probe and reference beams interfere with each other on the CMOS target, forming an off-axis hologram. As no pattern is displayed on the SLM, the hologram is recorded using the CMOS. By using the angular spectrum method, the recorded hologram is reconstructed to obtain the phase information of the speckle field [27–31], which is linearly calculated into grayscale and then displayed on the SLM to produce the phase-conjugate wavefront. A mirror  $M$ , located at the equivalent plane of the CMOS, is used to deliver the phase-conjugate wavefront back to the MMF. Finally, a charge coupled device (CCD) is used to record the phase-conjugate focus via an imaging system composed of the  $MO_2$  and Lens  $L_7$ .

First, we consider the case without masks in the module, which has been demonstrated in our recent works [27]. The probe beam after being focused by the  $MO_2$  forms a Gaussian focus, which is coupled near the fiber core axis. Due to modal scrambling, the speckle field is formed at the output facet of the fiber and then interferes with the reference beam to form an off-axis hologram, which is recorded using the CMOS. The phase information of the speckle field is reconstructed from the recorded hologram, as shown in Fig. 2(a1). The calculated phase conjugation pattern is displayed on the SLM to generate the phase-conjugate wavefront. To refocus at the original coupled spot, the phase-conjugate wavefront and original scattered wavefront must be precisely overlapped

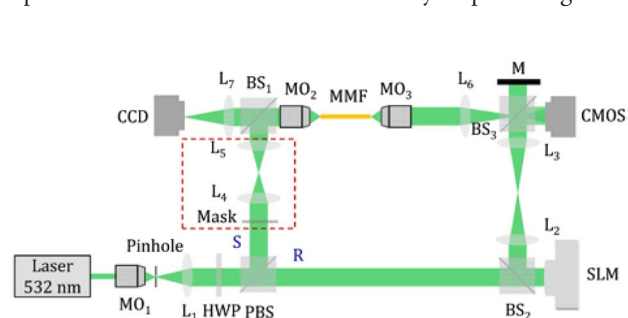


**Fig. 1.** Schematic of a DOPC system for regenerating structured laser beams.  $MO_1 - MO_3$ , microscope objectives;  $L_1 - L_7$ , lenses; HWP, half-wave plate; PBS, polarizing beam splitter;  $BS_1 - BS_3$ , beam splitters;  $M$ , mirror; SLM, spatial light modulator; CMOS, complementary metal oxide semiconductor; CCD, charge coupled device.

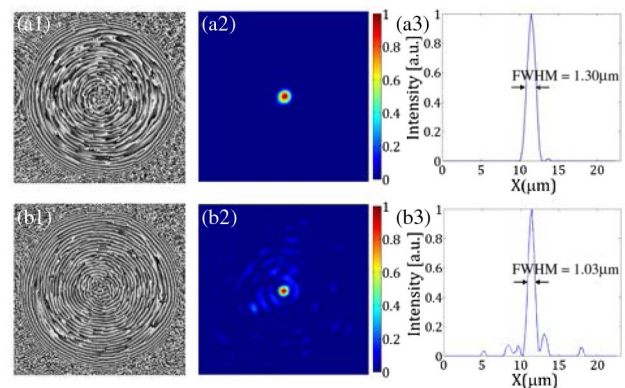


**Fig. 2.** Reconstruction results for focusing through a MMF based on DOPC. (a1)–(a3), (b1)–(b3) Results when a Gaussian and quasi-Bessel beam are focused into a MMF, respectively.

in the MMF, which is auto-corrected using the angular spectrum method [27,32]. As the probe beam is blocked, the phase-conjugate focus is recorded using the CCD, as shown in Fig. 2(a2). Its peak-to-background ratio (PBR), defined as the ratio between the maximum intensity of the focus and the mean intensity of the speckle field produced as no pattern is projected on the SLM, is evaluated at approximately 1200. Then, we demonstrate the capability of reconstructing a quasi-Bessel beam based on the time-reversal principle of DOPC. So far, a variety of methods have been proposed to produce quasi-Bessel beams [33–35]. Here, we adopt a relatively simple approach used in Ref. [33]. When a ring mask is placed in the module, the probe beam after being focused by the  $MO_2$  would produce a quasi-Bessel beam. Figure 2(b1) shows the reconstructed phase-conjugate image of the generated speckle field when the quasi-Bessel beam is coupled near the fiber core axis. Similarly, as the calculated phase conjugation pattern is displayed on the SLM, and the probe beam is blocked, we also observe a focus, as shown in Fig. 2(b2). The PBR of the conjugate focus is measured at approximately 300. To compare with the FWHM of the foci in Figs. 2(a2) and 2(b2), the corresponding intensity profiles along the horizontal direction are separately given in Figs. 2(a3) and 2(b3). It can be seen that as the quasi-Bessel beam is coupled into the MMF, the conjugate focus has a smaller FWHM, which could be useful in the enhancement of the spatial resolution of MMF-based endoscopes.

The remarkable property of quasi-Bessel beams is non-diffracting or propagation invariant over a limited distance. Therefore, we expect that when the quasi-Bessel beam is coupled into the MMF, the phase-conjugate focus could also show the property of a longer depth of field than a Gaussian focus. In Fig. 1, the  $MO_2$  is mounted on a three-dimensional stage with a resolution of  $1\ \mu\text{m}$ , which enables us to scan both sides of the focal plane along the beam propagation direction ( $z$ -axis). Here, a series of focal intensity images along the  $z$ -axis are recorded using the CCD by scanning the  $MO_2$ . Figures 3(a) and 3(b) separately give the reconstructed normalized intensity distribution in the  $y-z$  plane of the foci as shown in Figs. 2(a2) and 2(b2). As expected, when the quasi-Bessel beam is coupled into the MMF, the conjugate focus maintains propagation invariant over a limited distance. In other words, we have demonstrated the reconstruction of a quasi-Bessel beam through a MMF. The intensity profiles along the  $z$ -axis of the Gaussian and quasi-Bessel foci are given in Fig. 3(c). It can be seen that

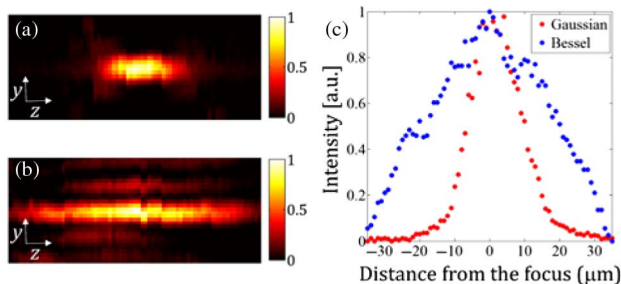


**Fig. 3.** Measurement results of the depth of field for the regenerated Gaussian focus and quasi-Bessel beam based on DOPC. (a), (b) Normalized intensity distribution in the  $y-z$  plane of the foci as shown in Figs. 2(a2) and 2(b2). (c) Intensity profiles along the  $z$ -axis of the Figs. 2(a) and 2(b).

the regenerated quasi Bessel beam has a depth of field about two times longer than the Gaussian focus.

Finally, we demonstrate the reconstruction of vortex beams, a kind of singular beams. To produce a vortex beam, a photomask-encoded desired spiral phase is placed in the module, which was used in our previous work [36]. As the probe beam illuminates the photomask, a vortex beam could be produced by spatially filtering the  $+1$  diffraction order via the  $4f$  system composed of Lenses  $L_4$  and  $L_5$ . First, we investigate a vortex beam with TC of 1 coupled into the MMF. The phase information of the speckle field generated through the MMF is reconstructed and then calculated into grayscale. When the phase conjugation pattern is projected on the SLM, and the probe beam is blocked, the phase-conjugate focus with a donut-like intensity distribution is regenerated and recorded using the CCD, as shown in Fig. 4(a1). To verify that the regenerated focus is a form of a vortex beam, we adopt the astigmatic transformation method to measure the beam TC by using a cylindrical lens [37,38]. Here, a flip mirror, cylindrical lens, another lens, and CCD (not given in Fig. 1) are added in the experimental setup. The flip mirror is placed between the Lenses  $L_4$  and  $L_5$ . After being reflected by the flip mirror, the conjugate beam through the lens and cylindrical lens is transformed into an astigmatic beam. The added CCD placed near the focal plane of the cylindrical lens is used to record the astigmatic transformation pattern, as shown in Fig. 4(a2). It can be seen that the transformation pattern has one dark stripe, which indicates that the conjugate focus is a vortex beam with TC of 1. Then, we further investigate a vortex beam with TC of 2 coupled into the MMF. The phase-conjugate focus is presented in Fig. 4(b1). Figure 4(b2) gives the corresponding astigmatic transformation pattern with two dark stripes, characterized by a vortex beam with TC of 2. Therefore, we prove without ambiguity that vortex beams through a MMF are regenerated based on DOPC, despite that only the phase of the original speckle field is time reversed. It can be seen that the vortex beams regenerated through the MMF based on DOPC are actually not perfect. The main factors might be the misalignment of the

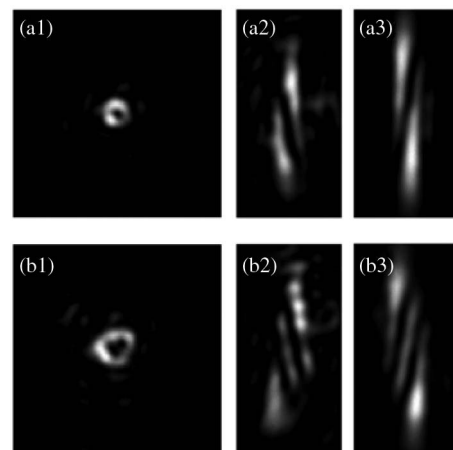


**Fig. 4.** Results for the regeneration of vortex beams through a MMF based on DOPC. (a1), (b1) Regenerated vortex beams with TCs of 1 and 2, respectively. (a2), (b2) Astigmatic transformation patterns corresponding to (a1) and (b1). (a3), (b3) Astigmatic transformation patterns of the vortex beams with TCs of 1 and 2, produced from the photomask, respectively.

DOPC system, the imperfection of the used phase-only SLM, as well as the coupled angle of vortex beams relative to the MMF cross section. In addition, by rotating the added flip mirror, the astigmatic transformation patterns of the corresponding vortex beams produced from the photomask could be recorded, as presented in Figs. 4(a3) and 4(b3), respectively. As can be seen, the stripes are tilted in the opposite orientation to those in Figs. 4(a2) and 4(b2), which indicates that the regenerated vortex beams through the MMF carry the opposite TC with respect to original vortex beams. In other words, the vortex beams regenerated through the MMF based on DOPC are indeed phase conjugate to the corresponding input vortex beams. In addition, the reconstruction of vortex beams could prove the fidelity of DOPC both in amplitude and phase, which indicates that DOPC has the ability to achieve three-dimensional imaging through complex media. Due to DOPC's shortest response time per degree of freedom, our method could also be developed to regenerate structured laser beams through dynamic scattering media, which remains a great challenge for other wavefront-shaping techniques. Moreover, if a full-polarization DOPC system is employed, the reconstruction of arbitrary structured laser beams, such as vector beams with space-variant polarization distribution, through complex media could be expected [39,40].

In conclusion, we have demonstrated a method for the reconstruction of a quasi-Bessel beam and vortex beams through a MMF based on DOPC. The regenerated quasi-Bessel beam shows the properties of a smaller FWHM and a longer depth of field with respect to a Gaussian beam, which could be used to improve the imaging resolution and depth of MMF-based endoscopes. The regeneration of vortex beams with TCs of 1 and 2 is confirmed by using the astigmatic transformation method, although only the phase of the original scattered field is time reversed. In addition, the regenerated vortex beams could show the fidelity of DOPC both in amplitude and phase through complex media. Moreover, compared with the astigmatic transformation patterns between the regenerated vortex beams and the corresponding input vortex beams, we could prove that the reconstruction results of DOPC through complex media are indeed phase conjugate to the input targets, which is experimentally demonstrated for the first time, to the best of our knowledge. While we demonstrate the reconstruction of structured laser beams through a MMF, these results could readily be demonstrated through other complex media, even including dynamic scattering media, which might open up new opportunities in some areas, such as super-resolution imaging and optical micromanipulation.

**Funding.** National Natural Science Foundation of China (NSFC) (11634010, 11774289, 61675170); Joint Fund of the National Natural Science Foundations of China and China Academy of Engineering Physics (CAEP) (U1730137); National Key R&D Program (2016YFA0300903, 2017YFA0303801); Beijing Graphene Innovation Program (Z161100002116028); National Equipment Project (ZDYZ2015-1).

## REFERENCES

1. A. P. Mosk, A. Lagendijk, G. Lerosey, and M. Fink, *Nat. Photonics* **6**, 283 (2012).
2. S. Rotter and S. Gigan, *Rev. Mod. Phys.* **89**, 015005 (2017).
3. S. M. Popoff, G. Lerosey, R. Carminati, M. Fink, A. C. Boccara, and S. Gigan, *Phys. Rev. Lett.* **104**, 100601 (2010).
4. I. M. Vellekoop and A. P. Mosk, *Opt. Lett.* **32**, 2309 (2007).
5. I. M. Vellekoop, A. Lagendijk, and A. P. Mosk, *Nat. Photonics* **4**, 320 (2010).
6. Z. Yaqoob, D. Psaltis, M. S. Feld, and C. Yang, *Nat. Photonics* **2**, 110 (2008).
7. M. Cui and C. Yang, *Opt. Express* **18**, 3444 (2010).
8. C. L. Hsieh, Y. Pu, R. Grange, and D. Psaltis, *Opt. Express* **18**, 12283 (2010).
9. C. L. Hsieh, Y. Pu, R. Grange, G. Laporte, and D. Psaltis, *Opt. Express* **18**, 20723 (2010).
10. H. Yu, J. Park, K. Lee, J. Yoon, K. Kim, S. Lee, and Y. Park, *Curr. Appl. Phys.* **15**, 632 (2015).
11. I. M. Vellekoop, M. Cui, and C. Yang, *Appl. Phys. Lett.* **101**, 081108 (2012).
12. I. N. Papadopoulos, S. Farahi, C. Moser, and D. Psaltis, *Opt. Express* **20**, 10583 (2012).
13. I. N. Papadopoulos, S. Farahi, C. Moser, and D. Psaltis, *Opt. Lett.* **38**, 2776 (2013).
14. T. R. Hillman, T. Yamauchi, W. Choi, R. R. Dasari, M. S. Feld, Y. Park, and Z. Yaqoob, *Sci. Rep.* **3**, 1909 (2013).
15. D. Wang, E. H. Zhou, J. Brake, H. Ruan, M. Jang, and C. Yang, *Optica* **2**, 728 (2015).
16. C. Ma, F. Zhou, Y. Liu, and L. V. Wang, *Optica* **2**, 869 (2015).
17. K. Lee, J. Lee, J. H. Park, J. H. Park, and Y. Park, *Phys. Rev. Lett.* **115**, 153902 (2015).
18. R. Horstmeyer, H. Ruan, and C. Yang, *Nat. Photonics* **9**, 563 (2015).
19. M. Duocastella and C. B. Arnold, *Laser Photon. Rev.* **6**, 607 (2012).
20. A. M. Yao and M. J. Padgett, *Adv. Opt. Photon.* **3**, 161 (2011).
21. Q. Zhan, *Adv. Opt. Photon.* **1**, 1 (2009).
22. D. L. Andrews, *Structured Light and Its Applications* (Academic, 2008).
23. D. Di Battista, D. Ancora, M. Leonetti, and G. Zacharakis, *Appl. Phys. Lett.* **109**, 121110 (2016).
24. T. Cizmar and K. Dholakia, *Nat. Commun.* **3**, 1027 (2012).
25. A. Boniface, M. Mounaix, B. Blochet, R. Piestun, and S. Gigan, *Optica* **4**, 54 (2017).
26. Y. Y. Xie, B. Y. Wang, Z. J. Cheng, Q. Y. Yue, and C. S. Guo, *Appl. Phys. Lett.* **110**, 221105 (2017).
27. C. Ma, J. Di, Y. Li, F. Xiao, J. Zhang, K. Liu, X. Bai, and J. Zhao, *Appl. Phys. Express* **11**, 062501 (2018).
28. W. Sun, J. Zhao, J. Di, Q. Wang, and L. Wang, *Opt. Express* **17**, 20342 (2009).
29. C. Ma, J. Di, J. Zhang, Y. Li, T. Xi, E. Li, and J. Zhao, *Appl. Opt.* **55**, 9435 (2016).
30. C. Ma, Y. Li, J. Zhang, P. Li, T. Xi, J. Di, and J. Zhao, *Opt. Express* **25**, 13659 (2017).
31. J. Zhang, S. Dai, C. Ma, J. Di, and J. Zhao, *Opt. Lett.* **42**, 3462 (2017).
32. M. Jang, H. Ruan, H. Zhou, B. Judkewitz, and C. Yang, *Opt. Express* **22**, 14054 (2014).
33. J. Durnin, J. Miceli, Jr., and J. H. Eberly, *Phys. Rev. Lett.* **58**, 1499 (1987).
34. D. McGloin and K. Dholakia, *Contemp. Phys.* **46**, 15 (2005).
35. P. Li, Y. Zhang, S. Liu, L. Han, H. Cheng, F. Yu, and J. Zhao, *Opt. Lett.* **41**, 4811 (2016).
36. Y. Zhang, X. Guo, L. Han, P. Li, S. Liu, H. Cheng, and J. Zhao, *Opt. Express* **25**, 25725 (2017).
37. Y. Peng, X. Gan, P. Ju, Y. Wang, and J. Zhao, *Chin. Phys. Lett.* **32**, 024201 (2015).
38. B. Y. Wei, P. Chen, S. J. Ge, W. Duan, W. Hu, and Y. Q. Lu, *Appl. Phys. Lett.* **109**, 121105 (2016).
39. Y. Shen, Y. Liu, C. Ma, and L. V. Wang, *Opt. Lett.* **41**, 1130 (2016).
40. S. X. Qian, Y. Li, L. J. Kong, C. H. Tu, and H. T. Wang, *Opt. Lett.* **39**, 4907 (2014).